



Contents lists available at SciVerse ScienceDirect

Mathematical and Computer Modelling

journal homepage: www.elsevier.com/locate/mcm

Assimilation of MODIS-LAI into the WOFOST model for forecasting regional winter wheat yield

Guannan Ma^a, Jianxi Huang^{a,*}, Wenbin Wu^b, Jinlong Fan^c, Jinqiu Zou^b, Sijie Wu^d^a College of Information and Electrical Engineering, China Agricultural University, Beijing, 100083, China^b Institute of Agricultural Resources and Regional Planning, Chinese Academy of Agricultural Sciences, Beijing, 100081, China^c National Satellite Meteorological Center, China Meteorological Administration, Beijing, 100081, China^d School of Geosciences and Info-Physics, Central South University, Changsha, 410083, China

ARTICLE INFO

Article history:

Received 27 September 2011

Accepted 27 October 2011

Keywords:

Remote sensing
Crop growth model
Sensitivity analysis
Data assimilation
Yield

ABSTRACT

Crop growth models have been applied successfully in forecasting crop yield at a local scale, while satellite remote sensing has the advantage of retrieving regional crop parameters. The new assimilation method of integrating the crop growth model with remote sensing has presented great potential in regional crop yield assessment. In this study, the Moderate Resolution Imaging Spectrometer (MODIS) leaf area index (LAI) data product was assimilated into the World Food Studies (WOFOST) crop growth model. Using the Extended Fourier Amplitude Sensitivity Test (EFAST) global sensitivity analysis approach, several local and regional crop parameters were identified to be recalibrated. The Shuffled Complex Evolution (SCE) optimization algorithm was used to estimate the emergence date, initial biomass and initial available soil water by minimizing the differences between the corrected MODIS-LAI and simulated LAI. Results indicated that the accuracy of water-limited crop yield was improved significantly after the assimilation. The root mean square error (RMSE) reduced from 983 kg/ha to 474 kg/ha and 667 kg/ha respectively in two different optimization schemes.

© 2011 Elsevier Ltd. All rights reserved.

1. Introduction

Crop yield is vital for agricultural production management. Traditional yield estimation is usually carried out through either sampling field measurements or agro-meteorological model forecasting. However, these methods are costly and time-consuming. In predicting regional crop yield effectively, integrating remotely sensed data into the crop growth model has great advantage when compared to the traditional methods [1]. Crop growth models, based on system analysis and computer simulation techniques, can dynamically describe the fundamental processes such as photosynthesis, respiration, biomass partitioning and soil water balance. Due to the rapidness and macro-view of remote sensing, empirical relationships between crop yield and remotely sensed signals (e.g. vegetation index) were often used in earlier studies.

Therefore, coupling remote sensing and the crop growth model provides a promising way to estimate the regional yield accurately. There are mainly two strategies based on data assimilation. The first strategy, with the objective to improve model performance, reinitializes crop model parameters by minimizing the differences between crop state variables simulated by the crop model and derived from remote sensing [2–6]. Dente et al. [7] assimilated the leaf area index retrieved from ENVISAT-ASAR and MERIS data into the CERES-wheat crop growth model over Matera site located in Southern Italy. After adjusting soil properties (wilting point and field capacity) and sowing date, results indicated that the root mean square

* Corresponding author. Tel.: +86 01062737628.
E-mail address: jxhuang@cau.edu.cn (J. Huang).

error (RMSE) of the yield maps ranged from 360 to 420 kg/ha. Xu et al. [8] reinitialized emergence date and minimum temperature of growth by comparing phenological information (green-up date and maturity date) extracted from MODIS-LAI data product and that from crop models, and the prediction results showed a better agreement with official statistical yields.

The second strategy, coupling a radiation transfer model to a crop model, directly compares remotely sensed reflectance with the simulated by the nested model so as to improve the precision of yield prediction [9–13]. Launay and Guerif [14] assimilated four to six SPOT and aerial photography data values into the SUCROS model, coupled with the scattering by arbitrarily inclined leaves (SAIL) reflectance model, and re-estimated crop establishment and root system settling parameters. The field-by-field yield estimates were improved with the relative root mean square error (RRMSE) decreased from 20% to about 10%. Ma et al. [15] coupled the WOFOST model to the SAIL-PROSPECT model through LAI in order to simulate soil adjusted vegetation index (SAVI). By means of the optimization algorithm (FSEOPT), emergence date and biomass at turn-green stage were re-initialized by minimizing the differences between simulated and synthesized SAVI from remotely sensed data. The results indicated that the spatial distribution of simulated weight of storage organ at the potential production level was more consistent to official yields.

In this paper, MODIS-LAI data was assimilated into the WOFOST crop growth model with the aim of predicting the yields in Hengshui, Hebei province of China. In view of the underestimation of MODIS-LAI due to the mixed pixel effect, and the contaminated pixel by the atmospheric condition, the LAI time series profile was smoothed with Savitzky–Golay filtering algorithm first. Then, the field measured LAI was used to correct MODIS-LAI data product, taking the original profile of MODIS-LAI into account. The local and regional parameters were chosen to be recalibrated through a global sensitivity analysis approach. The next part illustrated the data assimilation procedure based on an SCE optimization algorithm. These key methods were described in Section 2. Section 3 mainly presented the results with and without assimilation at the water-limited level, and evaluated the accuracy of yield subsequently. Conclusions were summarized in the last section.

2. Materials and methods

2.1. Study area

The study was conducted in Hengshui city (115°10'E–116°34'E, 37°03'N–38°23'N), Hebei province of China. Hengshui region, covering 8815 km² in total, consists of 11 counties, and the topography is characterized by alluvial plains. The climate of the area is continental monsoon with an average annual rainfall approximately ranging from 400 to 700 mm and temperature varying from 9 to 15 °C. Winter wheat, one of the staple food crops in this region, is generally planted in the beginning of October, turns green between the end of February and the beginning of March, flowers between the end of April and the beginning of May, and harvested in June. Fig. 1 shows the study area and the distribution of the field measurement sites.

2.2. Data preparation

2.2.1. Field observation data

Field observation was conducted to obtain the important agronomic and biological parameters of winter wheat during the entire growing season in the study area in 2008. The measurements mainly included crop varieties, plant height, LAI of different phenological stages (emergence, green-up and anthesis) measured by the LAI-2000 instrument, as well as soil moisture by TSC-I. Official statistical yield data in 2008 was also collected.

2.2.2. Remotely sensed data

MODIS-LAI data product (MOD15) of 2007 and 2008 during the growing season were employed in this study. Due to cloud or atmospheric contamination, the LAI time series profile presented an unsmoothed and jagged profile. For this reason, the Savitzky–Golay filtering algorithm [16] was applied to smooth MODIS-LAI data. Fig. 2 shows an example of LAI time series profile before and after S–G filtering.

Compared with the field measured LAI, MODIS-LAI data filtered by S–G algorithm were still low. A pixel with 1 km resolution in North China is always a mix of various land cover types, more than just winter wheat, which caused bad quality of LAI retrieved from MODIS data. Therefore, this research substituted MODIS-LAI with the LAI of field measurements, and fitted the LAI curve from 1 January 2008 (DOY: 1) to 7 May 2008 (DOY: 129) into the logistic function to correct the MODIS-LAI image. Consequently, the corrected LAI data were closer to the actual values. Fig. 3 shows the MODIS-LAI image before and after correction.

2.2.3. Climate, soil and crop data

The WOFOST crop growth model has inputs of climate, soil and crop parameters [17]. Climate elements consist of daily maximum and minimum temperature, solar radiation, wind speed, vapor pressure and precipitation. These data were interpolated and regionalized by means of an inverse distance weighting (IDW) method. Soil attributive parameters, such as soil moisture content of saturated soil, soil moisture content at wilting point and soil moisture content at field capacity, were obtained according to the field experiments. Most crop properties were genetic, decided by crop varieties, thus, the

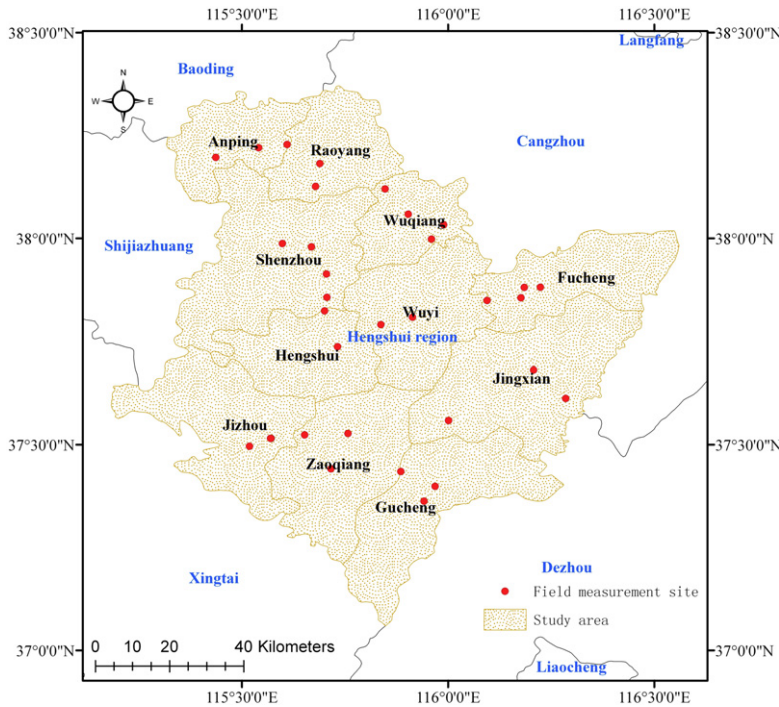


Fig. 1. Study area and field measurement sites.

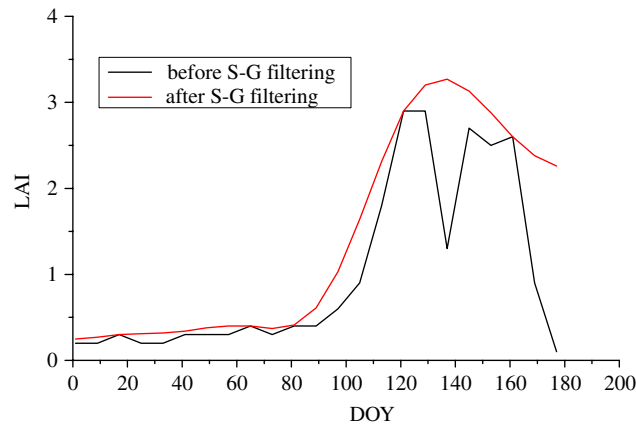


Fig. 2. LAI time series profile before and after S-G filtering.

acquisition of crop parameters could be done through the measurements and reviewing literature [12,8]. In addition, sowing date, the amount of irrigation and fertilization as management information were also collected and thermal accumulation in different growing stages was calculated from the meteorological station data.

2.3. Sensitivity analysis and crop model calibration

DSSAT series models of America and Wageningen series models of the Netherlands represent the development of crop growth models [18]. The WOFOST crop model, one of Wageningen series models, has a well description about the dynamic growing processes, for example, photosynthesis, respiration, biomass partitioning and soil water balance. The WOFOST model could simulate different crop varieties via adjusting input parameters at three levels (potential production level, water limited level and nutrition limited level). However, owing to long-term inheritance and cultivation, crops have become adapted to specific climate conditions and soil characteristics. Since the WOFOST model was developed mainly for Europe, most parameters need to be recalibrated before introducing the model into the study area, in order to simulate the whole growth period accurately. Selecting the sensitive parameters to be recalibrated was determined by the sensitivity analysis approach.

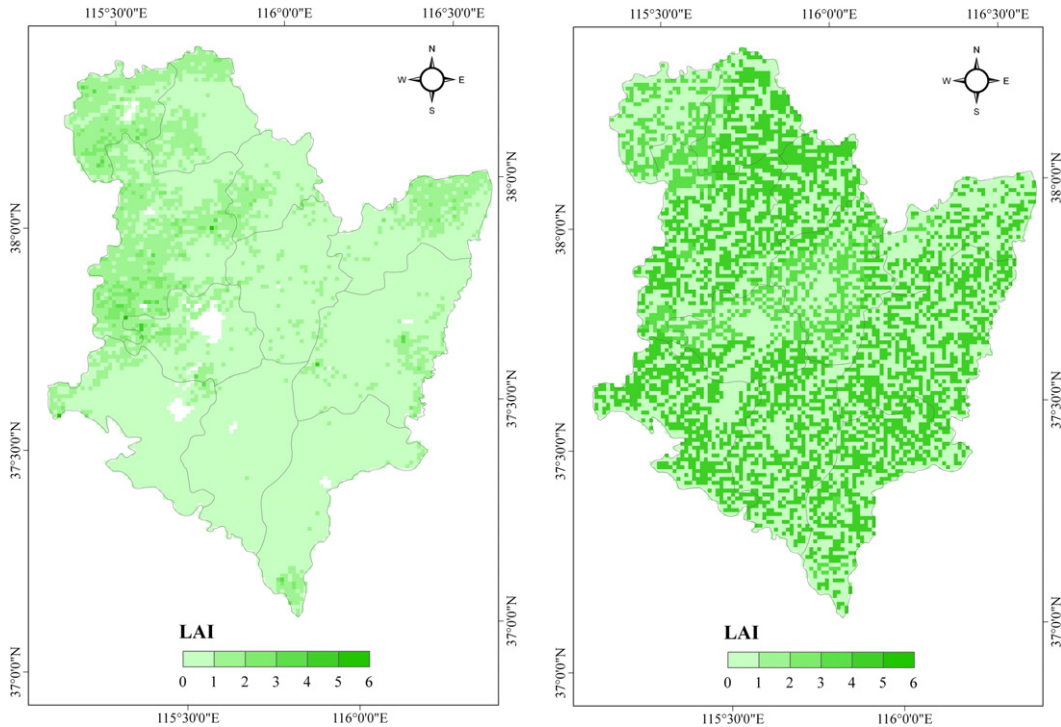


Fig. 3. MODIS-LAI image before and after correction (DOY: 129).

Table 1
Crop parameters.

| Parameter | Description | Range of value |
|-----------|---|----------------|
| TDWI | Initial total crop dry weight | 0.5–300 |
| LAIEM | Leaf area index at emergence | 0.0007–0.3 |
| RGRLAI | Max. relative increase in LAI | 0.007–0.5 |
| SLATB | Specific leaf area | 0.0007–0.0042 |
| SPAN | Life span of leaves growing at 35 °C | 17–50 |
| TBASE | Lower threshold temperature for aging of leaves | –10–10 |
| KDIFTB | Extinction coefficient for diffuse visible light | 0.44–1 |
| EFFTB | Initial light-use efficiency of CO ₂ assimilation of single leaves | 0.4–0.5 |
| AMAXTB | Maximum leaf CO ₂ assimilation rate | 1–70 |
| CVL | Conversion efficiency of assimilates into leaf | 0.6–0.76 |
| CVO | Conversion efficiency of assimilates into storage organ | 0.45–0.85 |
| CVR | Conversion efficiency of assimilates into root | 0.65–0.76 |
| CVS | Conversion efficiency of assimilates into stem | 0.63–0.76 |
| Q10 | Relative change in respiration rate per 10 °C temperature change | 1.5–2 |
| RML | Relative maintenance respiration rate leaves | 0.027–0.03 |
| RMO | Relative maintenance respiration rate storage organs | 0.003–0.017 |
| RMR | Relative maintenance respiration rate roots | 0.01–0.015 |
| RMS | Relative maintenance respiration rate stems | 0.015–0.02 |

Sensitivity analysis includes local sensitivity analysis and global sensitivity analysis. Local sensitivity analysis, also called one-at-a-time (OAT) approach, allows only one variable to change and fixes the others, considering the direct impact of each individual variable to the results. This approach omits the interactions among these variables. However, WOFOST is a multi-parameter nonlinear complex model, and the outputs reflect both the direct and indirect contributions of the parameters. In this paper, the Extended Fourier Amplitude Sensitivity Test (EFAST) [19–22] was used to evaluate the sensitivity of crop parameters (Table 1), soil and management parameters (Table 2).

Based on decomposition of the variance, an EFAST approach provides two sensitivity indexes: first-order and total sensitivity indexes. The first-order sensitivity index indicates the direct effect of the parameter to the model output, while the total sensitivity index with all input parameters varying simultaneously measures the sum of the direct and indirect contributions made by the test parameter to the model output. The total variance can be partitioned as

$$V(Y) = \sum_i V_i + \sum_{i \neq j} V_{ij} + \sum_{i \neq j \neq m} V_{ijm} + V_{12 \dots k}$$

Table 2
Soil and management parameters.

| Parameter | Description | Range of value |
|-----------|--|----------------|
| IDEM | Day of emergence | 275–305 |
| SMW | Soil moisture content at wilting point | 0.0832–0.1248 |
| SMFCF | Soil moisture content at field capacity | 0.24–0.36 |
| SMO | Soil moisture content of saturated soil | 0.328–0.492 |
| CRAIRC | Critical soil air content for aeration | 0.048–0.072 |
| KO | Hydraulic conductivity of saturated soil | 8–12 |
| SOPE | Maximum percolation rate root zone | 8–12 |
| KSUB | Maximum percolation rate of water to subsoil | 8–12 |
| WAV | Initial amount of available water in total rootable soil | 16–24 |
| DD | Depth of drainage | 16–24 |
| SMLIM | Maximum moisture content in topsoil | 0.052–0.078 |

where $V(Y)$ is the total variance of the model output, V_i is the variance of the parameter x_i , V_{ij} to $V_{12\dots k}$ is the variance of the interactions among these parameters. The first-order sensitivity index can be defined as

$$S_i = \frac{V_i}{V}.$$

Similarly, the second and third order sensitivity indexes can be defined as

$$S_{ij} = \frac{V_{ij}}{V} \quad S_{ijm} = \frac{V_{ijm}}{V}.$$

The total sensitivity index is the sum of all of the above indexes when i is included:

$$S_{T,i} = S_i + S_{ij} + S_{ijm} + \dots + S_{12\dots i\dots k}.$$

With the EFAST module of the professional sensitivity and uncertainty analysis software [23], the global sensitivity analysis of WOFOST parameters was realized. The experiment design consists of three steps as follows. The first step was to set the crop, soil and management parameters to follow uniform distribution in their individual range of value, and randomly sample 3000 and 1000 times respectively using the Monte Carlo method. In step 2, the generated combinations of parameters were input to the WOFOST model to simulate the yield of winter wheat. The last step was to calculate the first-order and total sensitivity indexes of each parameter, which is shown in Fig. 4.

It can be seen that AMAXTB, SPAN and CVO are most sensitive to yield with a total sensitivity index greater than 0.1. Meanwhile, parameters such as SLATB and TDWI also have a relatively high sensitivity. For the purpose of accurately simulating the crop growth processes, the parameters mentioned above were recalibrated through field measurements or referring to the predecessor's research [24,8]. The sensitivity analysis results of soil and management parameters indicate that SMO, WAV and IDEM are more sensitive to yield than the others, and this is an important reference for the assimilation procedure in the next section.

2.4. Assimilation method

The assimilation procedure adopted in this study minimized the cost function constructed by the corrected MODIS-LAI and simulated LAI. In order to obtain the optimal sets of parameters, the SCE optimization algorithm performed a re-initialization of the WOFOST crop growth model until the criterion threshold was satisfied (see Fig. 5).

SCE developed by Duan et al. [25] is based on the controlled random search, and incorporates competitive evolution and complex shuffling into numerical calculation, which improves the efficiency and performance for global optimization. The method was originally used in the hydrological models. Up until now, it has been proved that the combination of the SCE optimization algorithm and the crop model is feasible. The cost function in the SCE algorithm was constructed as follows:

$$J_{LAI} = \sum_{i=t_1}^{t_n} (LAI_{obs(t_i)} - LAI_{sim(t_i)})^2$$

where J is the value of the cost function, $LAI_{obs(t_i)}$ is the value of MODIS-LAI at time t_i , $LAI_{sim(t_i)}$ is the value of simulated LAI at time t_i , t_1 is the green-up date, and t_n is the maturity date. The SCE optimization algorithm is an iterative process, and it is thought to be successful when the absolute value of the difference among the latest cost function values in five loops converges to a predefined threshold.

3. Results

3.1. Re-initialization of model parameters

Previous papers [12,15,6], sensitivity analysis illustrated in Section 2.3, as well as the spatial variation of model parameters provided a valuable reference for selecting the parameters to be re-initialized at a regional scale. As thermal

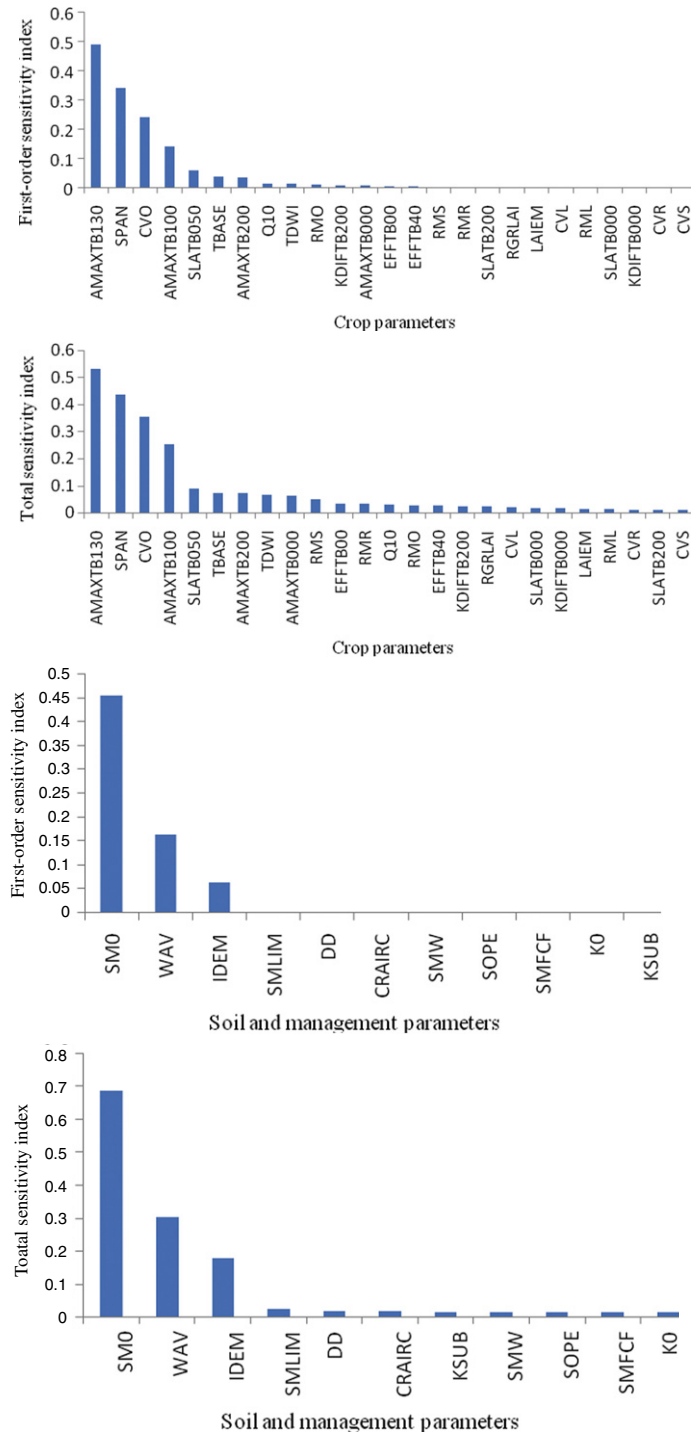


Fig. 4. Global sensitivity analysis.

accumulation, water supply and farming management in sowing period are quite different, emergence date, initial biomass and initial available soil water vary greatly. It is hard to obtain these parameters on a continuous temporal scale, furthermore, they are sensitive to crop yield, LAI and phenological information. Therefore, re-initializing the above three parameters improved the accuracy of yield assessment effectively. Two optimization schemes were carried out: only emergence date and initial biomass were re-initialized; all of the three parameters were re-initialized simultaneously. Table 3 lists the description and range of parameters to be optimized based on prior knowledge.

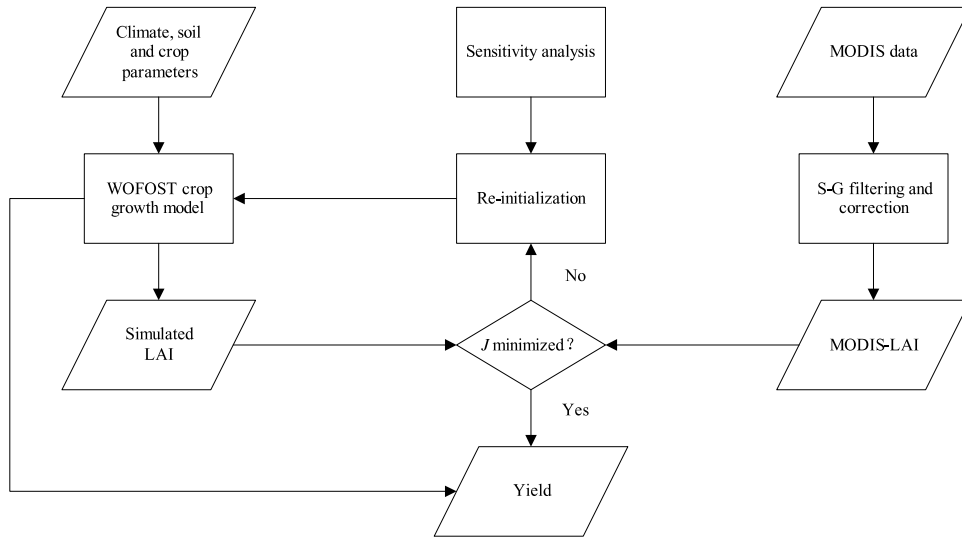


Fig. 5. Flow chart of assimilation procedure.

Table 3
Description and range of parameters to be optimized.

| Parameter | Description | Range of value |
|-----------|------------------------------|----------------|
| IDEM | Emergence date | 275–305 |
| TDWI | Initial biomass | 0–300 |
| WAV | Initial available soil water | 0–300 |

Table 4
Example of the SCE optimization process.

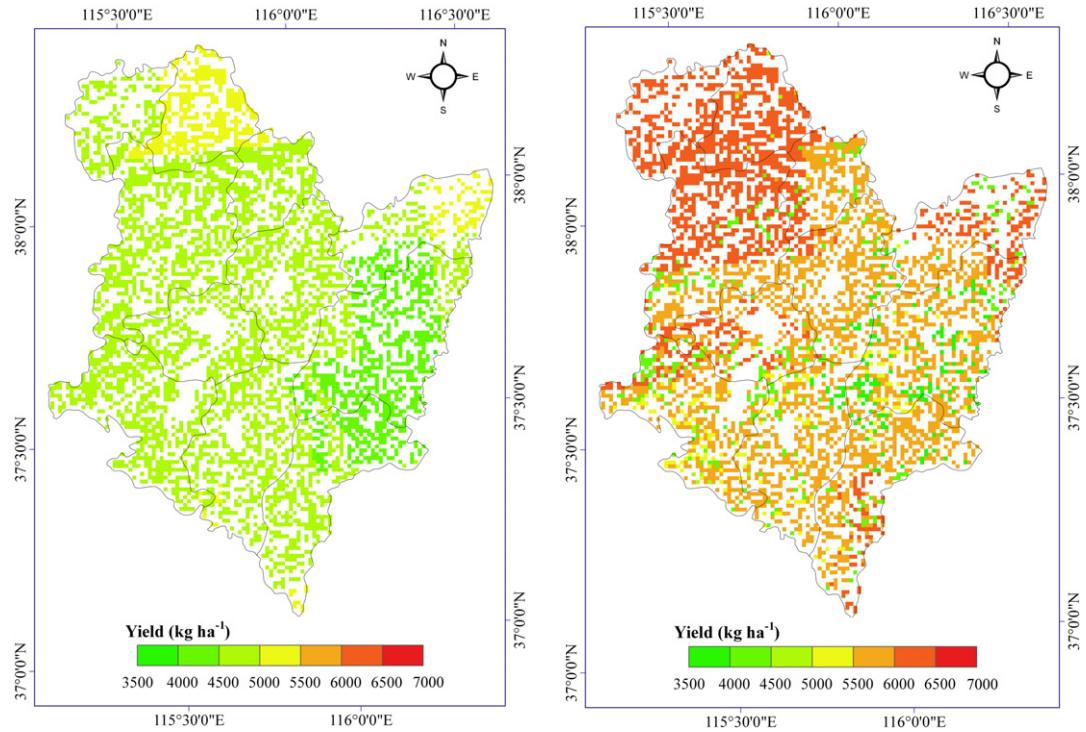
| Loop | Trials (scheme 1/ scheme 2) | Criterion (scheme 1/ scheme 2) | IDEM (scheme 1/ scheme 2) | TDWI (scheme 1/ scheme 2) | WAV |
|-----------|--------------------------------|-----------------------------------|------------------------------|------------------------------|-------|
| 0 | 10/14 | 98.8/38.5 | 294.6/276.5 | 5.9/20.6 | 122.4 |
| 1 | 21/32 | 43.2/38.5 | 282.8/276.5 | 28.5/20.6 | 122.4 |
| 2 | 34/53 | 38.1/38.0 | 282.9/288.0 | 23.1/17.7 | 196.6 |
| 3 | 47/76 | 38.0/37.9 | 283.4/279.9 | 20.7/19.3 | 186.3 |
| 4 | 64/98 | 37.8/37.8 | 285.5/287.0 | 21.4/18.4 | 179.0 |
| 5 | 82/121 | 37.8/37.8 | 285.5/285.7 | 21.7/18.7 | 181.0 |
| 6 | 97/143 | 37.8/37.8 | 286.4/285.7 | 21.7/18.7 | 181.0 |
| 7 | 114/163 | 37.8/37.8 | 286.1/286.0 | 21.6/18.7 | 182.6 |
| 8 | 131/183 | 37.8/37.8 | 286.3/285.5 | 21.7/18.6 | 180.4 |
| 9 | 146/202 | 37.8/37.8 | 286.3/288.9 | 21.7/18.6 | 194.3 |
| 10 | 163/226 | 37.8/37.8 | 286.3/291.6 | 21.7/18.7 | 198.6 |
| 11 | 180/247 | 37.8/37.8 | 287.6/289.5 | 21.7/18.7 | 193.4 |
| 12 | 197/272 | 37.8/37.8 | 286.5/291.0 | 21.7/18.7 | 199.3 |
| (Optimal) | | | | | |

3.2. Regional yield prediction

The WOFOST crop model, driven by regional climate, soil and crop data, simulated the LAI time series of each pixel during the growing season in 2008. The parameters were re-initialized in the two optimization schemes until the differences between the corrected LAI and simulated LAI were minimized (Table 4). Finally, running the WOFOST model again with the optimal sets of parameters, the yield distribution maps of winter wheat were obtained.

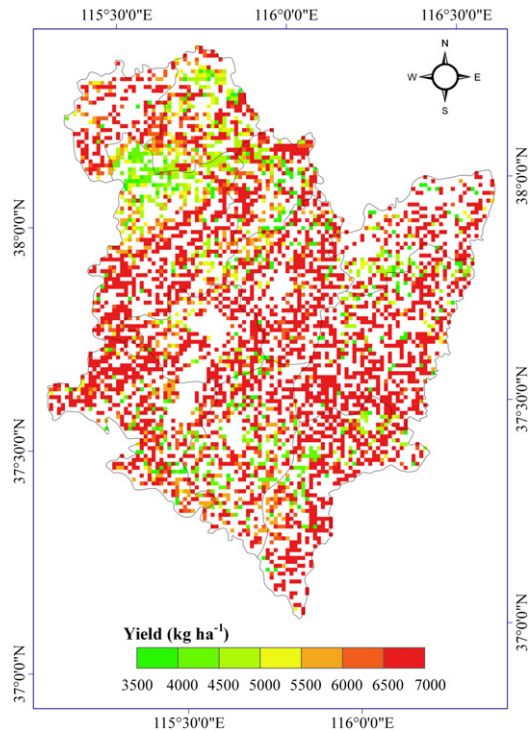
The emergence date (IDEM), initial biomass (TDWI) and initial available soil water (WAV) are optimized based on the J_{LAI} value. The criterion in each row is the best J_{LAI} value in each loop. The last row shows the final optimal values.

Fig. 6a shows the results of simulated yield without assimilation of remote sensing, while Fig. 6b and c are the yield distribution maps with assimilation of remote sensing in two different optimization schemes. The official statistical winter wheat yield at county level was used to evaluate the accuracy of the experimental results. It is evident that the simulated yield with assimilation has a moderate increase as a whole, and the yield of north parts is higher than the south, which is basically consistent with the trend of the official data. However, spatial variation of the yield is relatively low, which is partly caused by the small study area. In addition, multiple factors, such as climate, soil and management, influence the



(a) Without assimilation.

(b) With assimilation (scheme 1).



(c) With assimilation (scheme 2).

Fig. 6. Simulated winter wheat yield with and without assimilation (a. without assimilation b. with assimilation in the first scheme c. with assimilation in the second scheme).

Table 5
The error analysis of yield.

| | Mean (kg/ha) | Coefficient of determination (R^2) | Root Mean Square Error (RMSE, kg/ha) |
|------------------------------|--------------|--|--------------------------------------|
| Official statistical yield | 5648 | | |
| Without assimilation | 4781 | 0.015 | 983 |
| With assimilation (scheme 1) | 5748 | 0.326 | 474 |
| With assimilation (scheme 2) | 6382 | 0.189 | 667 |

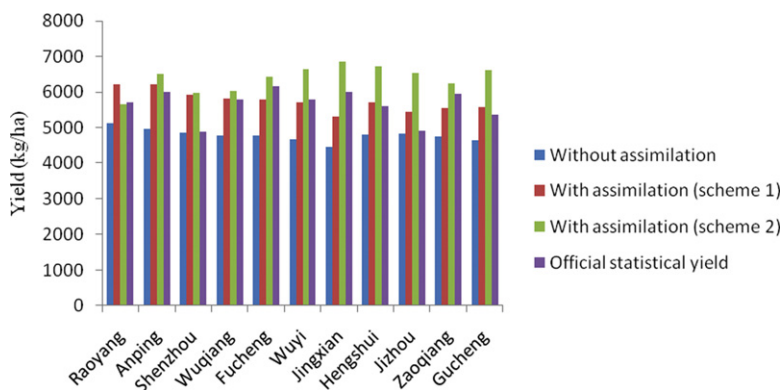


Fig. 7. Comparison of yield at county level.

yield formation jointly. The WOFOST crop model was driven by spatially varied climate data, and only a few crop and soil parameters, while the other parameters were fixed, which led to the small differences of simulated yield in study area consequentially. Table 5 shows the overall error analysis result of yield, and Fig. 7 compares the yield estimation at county level. It is thus clear that simulated yield with assimilation is well correlated with the official statistical yield. The root mean square error (RMSE) reduces to 474 kg/ha and 667 kg/ha respectively in two different optimization schemes. Except Shenzhou and Jizhou county, simulated yield of other counties are more accurate than without assimilation. The results indicate that assimilating MODIS-LAI into the WOFOST crop growth model by re-initializing the model parameters with the SCE optimization algorithm, improved the accuracy of the regional yield.

4. Conclusions and discussion

This paper presents a method based on the assimilation of MODIS-LAI into the WOFOST crop growth model. Local and regional model parameters to be recalibrated were selected through the EFAST global sensitivity analysis approach. Using the SCE optimization algorithm, emergence date, initial biomass and initial available soil water were then re-initialized by minimizing the differences between the simulated LAI and MODIS-LAI corrected with field measured LAI. This method was proved to be reliable with a significant improvement of the accuracy for forecasting the regional winter wheat yield.

In view of the disadvantages for the underestimation of MODIS-LAI, even though it was corrected with a field measured LAI, keeping the tendency of MODIS-LAI, the residual error resulted from the mixed pixel effect, still existed. Further work will focus on retrieving LAI using remotely sensed data with higher spatial and temporal resolution. The accuracy of simulated yield varied under different optimization schemes. The less the parameters to be re-initialized were, the faster and the better optimal sets of parameters were obtained. Scheme 2 added initial available soil water, on the contrary, the accuracy of simulated yield decreased moderately. Soil water balance is a dynamic process during the growing season, so that changing the initial conditions of soil moisture could not describe this dynamic process reasonably. The uncertainties regarding evapotranspiration (ET) and irrigation need to be further explored. For the purpose of obtaining a more accurate prediction of regional winter wheat yield, the crop model considering soil moisture time series and nutrition limitation during the growing season will be the research focus in the future.

In this study, LAI is the only connection between the crop growth model and remotely sensed data. If a crop model is coupled to a radiation transfer model (e.g. SAIL, ACRM), then assimilation of reflectance or vegetation index could be realized. Recently, assimilation of multi-objective variables (LAI, FAPAR, ET, soil moisture) has attracted more and more researchers' attention. Further work will focus on assimilating these variables simultaneously into the crop model with multi-objective optimization algorithms which reflect the influences of light, temperature and water on yield formation.

Acknowledgments

This study is supported by National Natural Science Foundation Project of China (No. 40901161), National Basic Research Program of China (No. 2010CB951504), National High Technology Research and Development Program 863 of China (No.2008AA10Z2) and Chinese Universities Scientific Fund (No. 2011JS142).

References

- [1] R. Macdonald, F. Hall, Global crop forecasting, *Science* 208 (1980) 670–679.
- [2] J.G.P.W. Clevers, H.J.C. van Leeuwen, Combined use of optical and microwave remote sensing data for crop growth monitoring, *Remote Sensing of Environment* 56 (1996) 42–51.
- [3] P.C. Doraiswamy, T.R. Sinclair, S. Hollinger, B. Akhmedov, A. Stern, J. Prueger, Application of MODIS derived parameters for regional crop yield assessment, *Remote Sensing of Environment* 97 (2005) 192–202.
- [4] Y. Yan, Q. Liu, Q. Liu, J. Li, L. Chen, Methodology of winter wheat yield prediction based on assimilation of remote sensing data with crop growth model, *Canadian Journal of Remote Sensing* 10 (5) (2006) 804–811.
- [5] H. Fang, S. Liang, G. Hoogenboom, J. Teasdale, M. Cavigelli, Corn- yield estimation through assimilation of remotely sensed data into the CSM–CERES–Maize model, *International Journal of Remote Sensing* 29 (10) (2008) 3011–3032.
- [6] J. Chen, J. Huang, H. Lin, Z. Pei, Rice yield estimation by assimilation remote sensing into crop growth model, *Science China* 40 (2010) 173–183.
- [7] L. Dente, G. Satalino, F. Mattia, M. Rinaldi, Assimilation of leaf area index derived from ASAR and MERIS data into CERES–Wheat model to map wheat yield, *Remote Sensing of Environment* 112 (4) (2008) 1395–1407.
- [8] W. Xu, H. Jiang, J. Huang, Regional crop yield assessment by combination of a crop growth model and phenology information derived from MODIS, *Sensor Letters* 9 (2011) 981–989.
- [9] M. Guerif, C. Duke, Calibration of the SUCROS emergence and early growth module for sugar beet using optical remote sensing data assimilation, *European Journal of Agronomy* 9 (1998) 127–136.
- [10] M. Weiss, D. Troufleau, F. Baret, Coupling canopy functioning and radiative transfer models for remote sensing data assimilation, *Agricultural and Forest Meteorology* 108 (2001) 113–128.
- [11] H. Bach, W. Mauser, Methods and examples for remote sensing data assimilation in land surface process modeling, *IEEE Transactions on Geoscience and Remote Sensing* 41 (2003) 1629–1637.
- [12] L. Zhang, S. Wang, Y. He, Y. Ma, L. Zhuang, Y. Hou, Winter wheat growth simulation under water stress by remote sensing in North China, *ACTA Agronomica Sinica* 33 (3) (2007) 401–410.
- [13] S. Yang, S. Shen, B. Li, B. Tan, Z. Li, Mapping rice yield based on assimilation of ASAR data with rice growth model, *Journal of Remote Sensing* 13 (2) (2009) 282–290.
- [14] M. Launay, M. Guerif, Assimilating remote sensing data into a crop model to improve predictive performance for spatial applications, *Agriculture Ecosystems and Environment* 111 (2005) 321–339.
- [15] Y. Ma, S. Wang, L. Zhang, Y. Hou, L. Zhuang, Y. He, F. Wang, Monitoring winter wheat growth in North China by combining a crop model and remote sensing data, *International Journal of Applied Earth Observation and Geoinformation* 10 (2008) 426–437.
- [16] J. Chen, P. Jonsson, M. Tamura, Z. Gu, B. Matsushita, L. Eklundh, A simple method for reconstructing a high-quality NDVI time-series data set based on the Savitzky–Golay filter, *Remote Sensing of Environment* 91 (2004) 332–344.
- [17] H.L. Boogaard, C.A. Van Diepen, R.P. Rotter, J.M.C.A. Cabrera, H.H. Van Laar, User's Guide for the WOFOST 7.1 Crop Growth Simulation Model and WOFOST Control Center 1.5, Wageningen (Netherlands), 1998, DLO Winand Staring Centre.
- [18] G. Hoogenboom, Contribution of agrometeorology to the simulation of crop production and its applications, *Agricultural and Forest Meteorology* 103 (12) (2000) 137–157.
- [19] A. Saltelli, S. Tarantola, K.P.S. Chan, A quantitative model-independent method for global sensitivity analysis of model output, *Technometrics* 41 (1) (1999) 39–56.
- [20] B. Matsushita, M. Xu, J. Chen, S. Kameyama, M. Tamura, Estimation of regional net primary productivity (NPP) using a process-based ecosystem model: How important is the accuracy of climate data? *Ecological Modeling* 178 (2004) 371–388.
- [21] J. Wu, F. Yu, Z. Chen, J. Chen, Global sensitivity analysis of growth simulation parameters of winter wheat based on EPIC model, *Transactions of the CSAE* 25 (7) (2009) 136–142.
- [22] Z. Jiang, Z. Chen, Q. Zhou, J. Ren, Global sensitivity analysis of CERES–Wheat model parameters, *Transactions of the CSAE* 27 (1) (2011) 236–242.
- [23] Simlab, Software package for uncertainty and sensitivity analysis, Joint Research Centre of the European Commission. Free downloadable at: <http://simlab.jrc.ec.europa.eu>, 2011.
- [24] D. Wu, Z. Ouyang, X. Zhao, Q. Yu, Y. Luo, The applicability research of WOFOST model in North China plain, *Acta Phytocologica Sinica* 27 (5) (2003) 594–602.
- [25] Q.Y. Duan, V.K. Gupta, S. Sorooshian, Shuffled complex evolution approach for effective and efficient global minimization, *Journal of Optimization Theory and Application* Plenum Publishing Corporation 76 (3) (1993) 501–521.